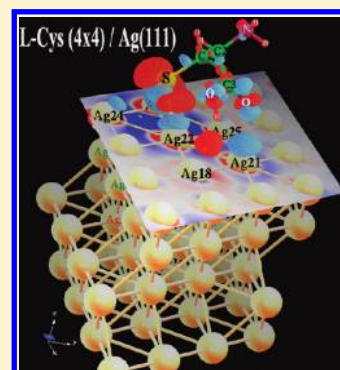


Ab Initio Studies of the Electronic Structure of L-Cysteine Adsorbed on Ag(111)

N. B. Luque,[‡] P. Vélez,[§] K. Pötting,[‡] and E. Santos^{*,†,‡}[†]Instituto de Física Enrique Gaviola (IFEG-CONICET), Facultad de Matemática, Astronomía y Física, Universidad Nacional de Córdoba, 5000 Córdoba, Argentina[‡]Institute of Theoretical Chemistry, Ulm University, D-89069 Ulm, Germany[§]Departamento de Matemática Física, Facultad de Ciencias Químicas, Universidad Nacional de Córdoba, 5000 Córdoba, Argentina

S Supporting Information

ABSTRACT: We have performed ab initio calculations for the adsorption of L-cysteine on Ag(111) using density functional theory. We have focused on two possible adsorbed species: the L-cysteine radical ($\bullet\text{S}-\text{CH}_2-\text{CH}-\text{NH}_2-\text{COOH}$) adsorbed almost flat at a bridge site, slightly displaced toward an fcc location, and the zwitterionic radical Z-cysteine ($\bullet\text{S}-\text{CH}_2-\text{CH}-\text{NH}_3^+-\text{COO}^-$) adsorbed at a bridge site, shifted to a hcp site forming a (4×4) unit cell ($\theta = 0.06$) and a $(\sqrt{3} \times \sqrt{3}) R 30^\circ$ unit cell ($\theta = 0.33$), respectively. Special attention has been paid to the electronic structure of the system. The adsorbate–silver bond formation has been exhaustively investigated by analyzing the density of states projected onto the different atoms of the molecule, and by charge density difference calculations. A complicated interplay between sp and d states of silver in the formation of bonds between the adsorbates and the surface has been found. The role of the carboxyl group in the interaction with the surface has been also analyzed.



INTRODUCTION

L-Cysteine is a special thiol molecule, which also contains amino and carboxyl groups. Its chemical structure is optimal to act as a linker between the surface of a metal and a biological environment. The three functional groups are able to interact with the metal surface. Several theoretical investigations of conformers have focused on the calculation of vibrational and rotational frequencies.^{1–6} In their pioneering work, Gronert and O'Hair¹ performed ab initio studies of 324 possible conformers of L-cysteine for the gas phase and identified 42 of them as stable or metastable. The energy of the conformers varies by about 0.4 eV, and in some cases several of them are within 0.1 eV of the global minimum, which involves structures where the carboxyl proton interacts with the amino group. Interactions between the carboxyl proton and the side-chain substituent SH are less favorable. A more recent investigation² took the 15 most stable structures obtained in ref 1 as starting points for structural optimization. The relative conformational energies obtained by these authors are also within 0.2 eV. Additionally, it is well-known that amino acids can exist as zwitterions in solutions and solid phase.⁶

The relative energy between the majorities of conformers of the “free molecule” is very close, as mentioned above. The internal flexibility of carboxyl and amine groups allows an easy rotation with respect to the backbone of the molecule. Thus, it is expected that the presence of a metallic surface affects the structure and dynamics to such an extent that a variety of adsorbates with a local minimum of energy are possible. There are in the literature both experimental and theoretical investigations of self-assembled monolayers (SAMs) on metal

surfaces formed from L-cysteine on diverse substrates. Here, we shall briefly mention the more relevant findings for the present work, focusing on the adsorption at silver and at gold.^{7–19} Most of the theoretical studies concerning energetic and electronic properties have been concerned with gold surfaces. Di Felice et al.^{13,14} have given a detailed description of the adsorption of L-cysteine on Au(111) using density functional theory (DFT). They employed a repeated $2\sqrt{3} \times 3$ supercell containing one adsorbed molecule, such that the resulting coverage was 0.082. The sulfur headgroup sitting at the bridge site appears as the most favorable configuration. They claimed that hybridization of the p-states of sulfur with the d-band of gold produces bonding and antibonding orbitals, both below the Fermi level. They have found that, under an appropriate configuration of the adsorbate, the amino functional group also contributes to the anchoring of the molecule as revealed by the changes observed in the p-electronic states of nitrogen. Kühnle et al.¹⁵ have performed DFT calculations of cysteine adsorbed on Au(110) surfaces, which indicate that the chiral specificity of the dimer formation process is driven by the optimization of three bonds on each cysteine molecule (sulfur–gold, amino–gold, and carboxylic–carboxylic). They also found that the bridge site is most favorable. Šljivančanin et al.¹⁶ have investigated the adsorption of cysteine on a chiral Au(17 11 9) surface by DFT and found that no enantio-specificity arises, since this molecule only binds to the gold surface through its

Received: March 14, 2012

Revised: May 5, 2012

Published: May 8, 2012

thiolate and amino groups, while the carboxyl group stays away from the surface. Theoretical studies carried out by Nazmutdinov and co-workers^{17,18} have shown that the optimized geometry for the adsorption of four L-cysteine forms (the molecule, the anion, the neutral radical, and its zwitterions) adsorbed at top, bridge, and 3-fold hollow sites of a planar Au₁₂ cluster is the radical adsorption on top. Recently, Höfiling et al.¹⁹ have investigated the single-molecule adsorption of cysteine at low coverage (4×4 supercell) on Au(110) by means of DFT. They have performed an exhaustive analysis of the electronics of the isolated bonds corresponding to the amino–gold and thiolate–gold bonds to the surface and for simultaneous bonding via both of these functional groups. Flat adsorption configurations with S–Au at an off-bridge site and NH₂–Au at an off-top site were found to be energetically favored. Recently, we have carried out an extensive study of the SAM formation from propanethiol on Au(111) surfaces²⁰ combining DFT calculations and our own theory for bond-breaking.²¹

Investigations of the adsorption of cysteine on silver surfaces are rather scarce. Jing and Fang²² have performed surface enhanced Raman spectroscopy (SERS) and DFT studies of the adsorption of L-cysteine on gold/silver nanoparticles and found different behavior. While in gold colloidal solution, L-cysteine molecules interacted with the gold surface simultaneously through sulfur, NH₃⁺, and COO[−] groups; in silver colloidal solution activated by coadsorption of chloride anions, the adsorption of two molecules led to the formation of one L-cysteine molecule by the S–S bond, and the molecules were attached to the silver surface via the carboxylate and amino groups. More recent experimental and theoretical studies performed by Diaz Fleming et al.²³ provide evidence that the COO[−], NH₃⁺, and SH groups are involved in the adsorption of the zwitterionic form of L-cysteine on silver nanoparticles. They also found that in solution the zwitterionic form has the tendency to form the corresponding dipeptide through the S–S bond, whereas in solid state and in the presence of metallic surfaces this tendency is reverted. Brolo et al.⁹ have investigated by SERS and second harmonic generation (SHG) the adsorption of L-cysteine on polycrystalline silver electrodes. They have observed a strong potential dependence of the conformation at the surface. At more positive potentials, where the coadsorption of chloride anions takes place, the carboxylate group is kept away from the surface, and the chloride interacts favorably with the protonated amino group and repels the carboxylate. When the potential is swept to negative values, the chloride ions leave the surface allowing a conformational change that brings the carboxylate group closer to the surface.

In our previous works,^{24,25} we have analyzed the behavior of L-cysteine SAMs on Ag(111) in an electrochemical environment by means of impedance spectroscopy, SHG, and DFT. The theoretical calculations were performed for the adsorption of an adlayer with the structure ($\sqrt{3} \times \sqrt{3}$) R 30° ($\theta = 0.33$), and we have found that, under particular conditions, zwitterionic species can be formed. When the hydrogen of the carboxyl group is oriented away from the surface and the initial C_α–S–Ag angle is almost flat, the formation of the zwitterion is probably caused by an intramolecular transfer of the proton from the carboxyl to the amine group. However, these transformations are not observed at lower coverage.

In the present contribution, we shall consider two particular systems corresponding to the more stable local minima at the lowest and the highest coverage (circles in Figure 1): the L-

cysteine radical ($\bullet\text{S}-\text{CH}_2-\text{CH}-\text{NH}_2-\text{COOH}$) adsorbed at a bridge site slightly displaced toward a fcc location, and the zwitterionic radical Z-cysteine ($\bullet\text{S}-\text{CH}_2-\text{CH}-\text{NH}_3^+-\text{COO}^-$) adsorbed at a bridge site shifted to a hcp site within a (4×4) unit cell ($\theta = 0.06$) and a ($\sqrt{3} \times \sqrt{3}$) R 30° unit cell ($\theta = 0.33$), respectively. For simplicity, and in order to facilitate the description, from now on we shall call them L-cys and Z-cys, respectively.

We shall investigate not only the energetic but also the electronic properties of these two adsorbates. The interaction with the electronic states of the substrate will be analyzed in detail for both different possible conformations.

METHODOLOGY

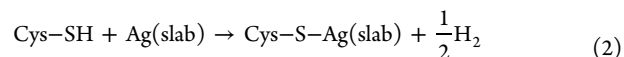
The methodology was similar to that employed in our previous work.²⁵ However, for clarity we summarize here a few details. We have employed the generalized gradient approximation (GGA) in the version of Perdew–Burke–Ernzerhof (PBE)²⁶ to perform DFT calculations as implemented in the SIESTA code version 3.^{27,28} It uses Troullier–Martins norm-conserving pseudopotentials²⁹ to represent the nucleus and core electrons of the considered species. The basis set used for the expansion of the Kohn–Sham eigenstates is composed of a set of numerical atomic orbitals including optionally polarization orbitals. An energy shift of 75 meV has been chosen as a compromise between accuracy and computational efficiency. We have taken an energy cutoff of 200 Ry and a double- ζ plus polarization orbital basis set (DZP). All geometries have been optimized until the force on each atom was less than 0.04 eV/Å. The ground state energy of the single L-cysteine molecule has been calculated using a ($20.85 \text{ Å} \times 20.85 \text{ Å} \times 62 \text{ Å}$) unit cell. The dimension of this cell is much larger than the amino acid itself; so the lateral interactions are expected to be rather small. We have modeled our system employing repeated supercells consisting of four (111) layers of silver atoms and a vacuum width of 20 Å. The fcc structure of the metal has been represented through a dense hexagonal packing (ABCA). We have used 12 k-points with respect to the surface unit cell for the Brillouin zone (BZ), and the calculated lattice constant for silver was $a = 4.19 \text{ Å}$. We have considered one L-cysteine radical adsorbed at one surface of the slab. According to the coverage to be investigated, each layer of the slab forms a supercell in the (111) plane with the corresponding overlayer structure (see Figures 2 and 3).

As mentioned in the Introduction, in the present contribution we choose two particular configurations corresponding to local minima of energy as shown in Figure 1. All atoms of L-cysteine and the two upper layers of the Ag slab have been allowed to relax in all directions. The position of the rest of the Ag atoms (two bottom layers) has been kept fixed. The adsorption energy E_{ads} can be calculated from

$$E_{\text{ads}} = E_{\text{system}} - (E_{\text{slab}} + E_{\text{Cys-Rad}}) \quad (1)$$

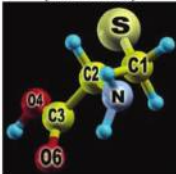
where E_{sys} is the total energy of the system and E_{slab} is the energy of the isolated metal slab with the two upper layers relaxed. The selection of the reference for the adsorbate could be ambiguous. On one hand, we can relax the L-cys radical or the Z-cys radical isolated from the metal within an equivalent cell as it is adsorbed on the surface (i.e., (4×4) and ($\sqrt{3} \times \sqrt{3}$) R 30°, respectively). On the other hand, we can choose the L-cys radical within a very large cell (i.e., (7×7)), where the intermolecular interactions are absent and relax this conformer.

Additionally, these values can be corrected adding the dissociation energy of L-cysteine to the radical and hydrogen atom in vacuum and subtracting the dissociation energy of a hydrogen molecule in order to obtain the energy corresponding to the global reaction:



The electronic redistribution due to metal–adsorbate interactions has been also investigated. This analysis can be performed comparing the results of two different approaches, the charge transfer between the

Table 1. Calculated Structural Parameters in Comparison with Experimental and Theoretical Data of the Literature^a

Bond - angles distances (Å-°) and torsion angles (°)	L-Cys-SH(gas) 3 most stables calculated structures from ref. [2] experimental values from ref [36] in parentheses, calculated structures from ref. [14]	L-Cys-S*(vac) (our results) 	L-Cys-S*/ Au(111) S _{bf} / NS _{bf} sites from ref.[14] (θ=0.08)	LCysS*/ Ag(111) (4x4) (our results) (see Figure 1) (θ=0.06)	Z-Cys-S*/ Ag(111) (√3x√3) (our results) (see Figure 1) (θ=0.33)	Z-Cys-SH (sol)/ Ag(cluster) from ref.[23]
S-Ag(sur)				1.888	1.898	2.948
S-Ag ₁₄ / Ag ₂₆			2.51/2.51	2.54	2.564	
S-Ag ₁₅ / Ag ₂₂			2.51/2.51	2.56	2.582	
S-Ag ₁₆ / Ag ₂₄				3.03	2.969	
O ₄ -Ag(sur)				4.447	4.447	2.597
O ₆ -Ag(sur)				2.439	6.110	2.597
O ₆ -Ag ₂₁				2.598	---	
N-Ag(sur)			/2.35	5.079	5.725	3.497
N-Ag ₂₅				5.40		
C ₁ -S-Ag(sur)			147/	139	142	
H _{10(O4)} -Ag(sur)				2.29		
H _{10(O4)} -Ag ₁₈				2.58		
C ₃ -O ₆	1.22; 1.26	1.23	1.23/1.23	1.23	1.28	1.251
C ₃ -O _{4(H)}	1.35; 1.37; 1.25	1.37	1.36/1.36	1.35	1.27	1.257
O ₄ -H	1.00; 0.98	0.98		0.99	1.54 (H in N)	
C ₃ -C ₂	1.55; 1.53; 1.53	1.54	1.54/1.52	1.54		1.573
C ₂ -N	1.47; 1.45; 1.49	1.46	1.47/1.47	1.47		1.512
N-H	1.02	1.03		1.03	1.04; 1.06; 1.09	1.034
C ₂ -C ₁	1.53; 1.55; 1.53	1.56	1.53/1.53	1.55	1.53	1.522
C ₁ -S	1.83; 1.82; 1.81	1.80	1.88/1.89	1.85	1.87	1.850
S-H	---	---	---	---	---	1.350
O ₄ -C ₃ -O ₆	126	123	124/124	123.9	126.5	130.8
C ₁ -C ₂ -C ₃	108.4; 112.1; 112	109.8	110/111	108.2	117.7	116.1
C ₁ -C ₂ -N	108.7; 113.8; 110	110.5	112/110	108.7	113.0	113.2
C ₂ -C ₁ -S	114	116.6	114/116	112.9	107.2	116.5
C ₁ -S-H	---	---	---	---	---	97.3
C ₃ -C ₂ -N	109	109.6	107/112	112.9	106.5	103.5
O ₆ -C ₃ -C ₂ -N	(-4)	-1.17	-47/-3	-57.6	49.0	43.7
O _{4(H)} -C ₃ -C ₂ -N	(177)	-179.7	133/176	122.0	-129.3	-132.9
O ₆ -C ₃ -C ₂ -C ₁	(117)	120.4	72/122	62.7	177.0	168.4
C ₃ -C ₂ -C ₁ -S	(84)	74.8	69/174	86.9	69.4	-59.1
N-C ₂ -C ₁ -S	(-156)	-164.2	-169/-63	-175.2	-165.8	60.5
C ₂ -C ₁ -S-H	---	---	---	---	---	-100.6
H-O ₄ -C ₃ -C ₂		177.6	---	172.3	---	---

^aSecond column, molecule in the phase gas; third column, radical in vacuum; fourth column, radical adsorbed on two different sites of Au(111) surface at a coverage of 0.08 ($3 \times 2\sqrt{3}$ cell); fifth column, radical adsorbed on Ag(111) surface at a coverage of 0.06 (4×4 cell); sixth column, cysteine zwitterion radical adsorbed on Ag(111) surface at a coverage of 0.33 ($\sqrt{3} \times \sqrt{3}R30^\circ$ cell); seventh column, cysteine zwitterion on a Ag (18-atoms-cluster representing the (110) surface). Bond lengths are in Å, and angles in degrees. For distinguishing between the different adsorbates, see references and Figure 2.

adsorbate and the substrate as well as the formation of chemical bonds between them. The charge density difference, $\Delta n(r)$ is defined as³⁰

$$\Delta n(r) = n_{\text{Ads-Sub}}(r) - [n_{\text{Sub}}(r) + n_{\text{Ads}}(r)] \quad (3)$$

where $n_{\text{Ads-Sub}}$ is the electron charge density distribution of the whole system at its final state, n_{Sub} and n_{Ads} are the electron charge density distribution for the isolated substrate and adsorbate, respectively, but with the fixed final configuration upon adsorption. The density of electronic states (DOS) of the system has also been calculated, and the projection onto different individual atomic orbitals (PDOS) has been analyzed. The electronic redistribution due to metal-adsorbate interactions has been also analyzed comparing the PDOS with respect to those of the adsorbing species in absence of the metal. Here the geometric structure of the isolated species has also been kept the same as in the combined system. The energy alignment between both systems has been obtained by determining the Fermi level self-consistently using the vacuum level of the electrostatic potential. The energy zero is set to the Fermi level of the metal. The density of states was normalized to one in all cases. The molecular graphics have been done with the XCRYSDEN package.³¹

RESULTS AND DISCUSSION

Choice of Two Characteristic Adsorbates for Detailed Analysis.

As pointed out in the Introduction, a variety of conformers of the cysteine molecule can exist depending on the environment and the inter- and intramolecular interactions. We have chosen one of them, whose geometrical parameters are given in Table 1. When the molecule approaches the surface of silver, depending on the initial orientation, various stable adsorbates can be obtained. Figure 1 shows typical results for the energetics of the adsorbed L-cysteine radical on the Ag(111) surface at different coverage and diverse starting structures on different sites (top, bridge, fcc, and hcp). Here the position of the sulfur atom has been kept fixed in the x and y coordinates in order to distinguish the energy difference between different sites.

In all cases, stable local minima have been found. The magnitude of the adsorption energy decreases almost linearly with increasing coverage for all structures, indicating a

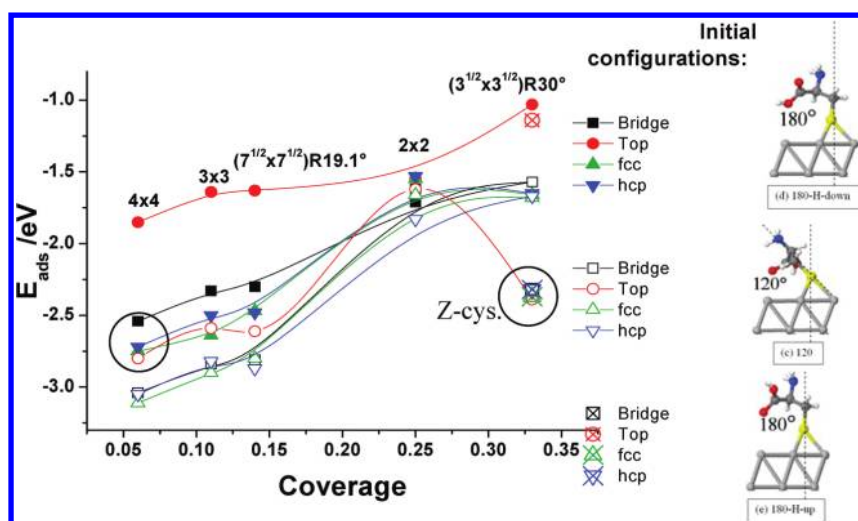


Figure 1. Dependence on the coverage of the bonding energy of L-cysteine adsorbed at the silver surface on different sites (as indicated in the plot). Three different initial configurations were employed: where the angle $C_\alpha-S-Ag$ was 180° with the hydrogen of the carboxyl group oriented “downwards” (full symbols), where the angle $C_\alpha-S-Ag$ was 120° (open symbols), and where the angle $C_\alpha-S-Ag$ was 180° with the hydrogen of the carboxyl group oriented “upwards” (crossed symbols).

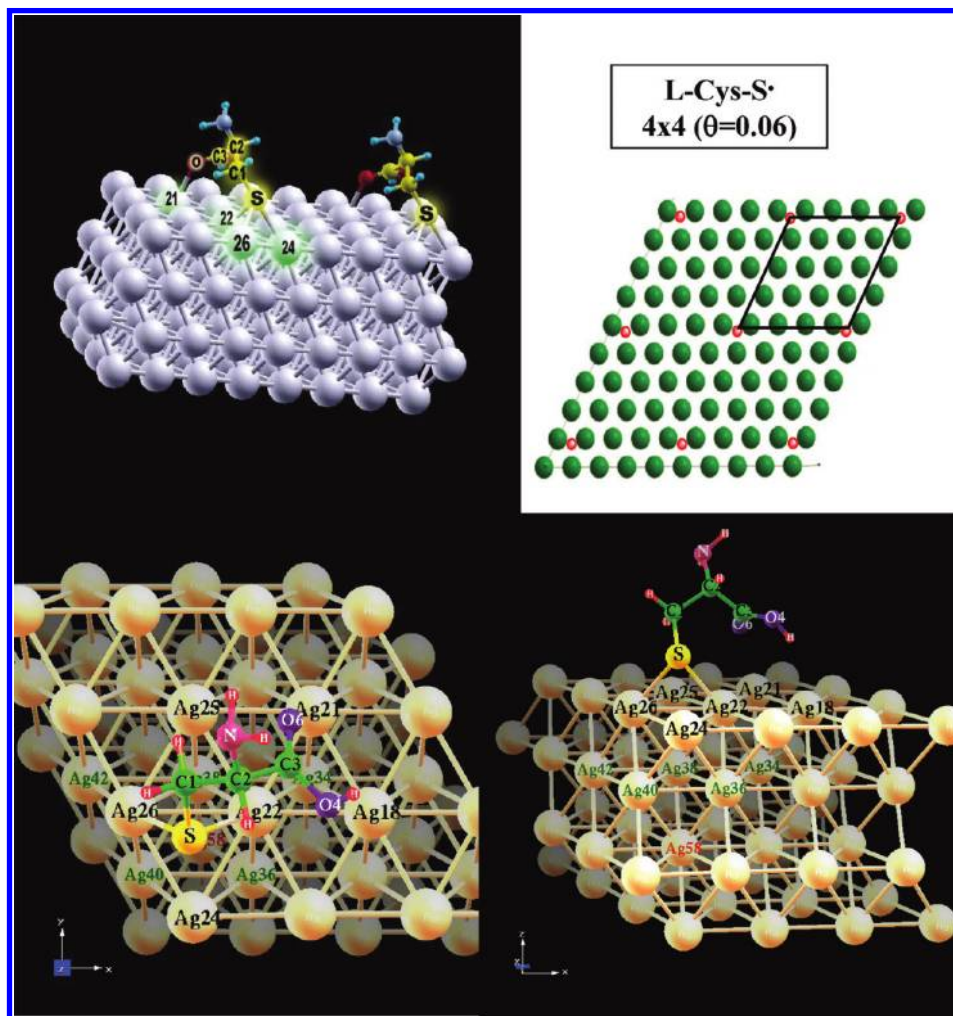


Figure 2. Different 3D views of the relaxed system corresponding to L-cys adsorbed at a bridge site shifted toward fcc sites ($\theta = 0.06$). The silver atoms of the three upper layers interacting more strongly with the adsorbate are labeled with numbers (in black those of the top layer, in green those of the second layer, and in red the atom of the third layer just below the sulfur atom). The unit cell (4×4) used for the calculations is also shown.

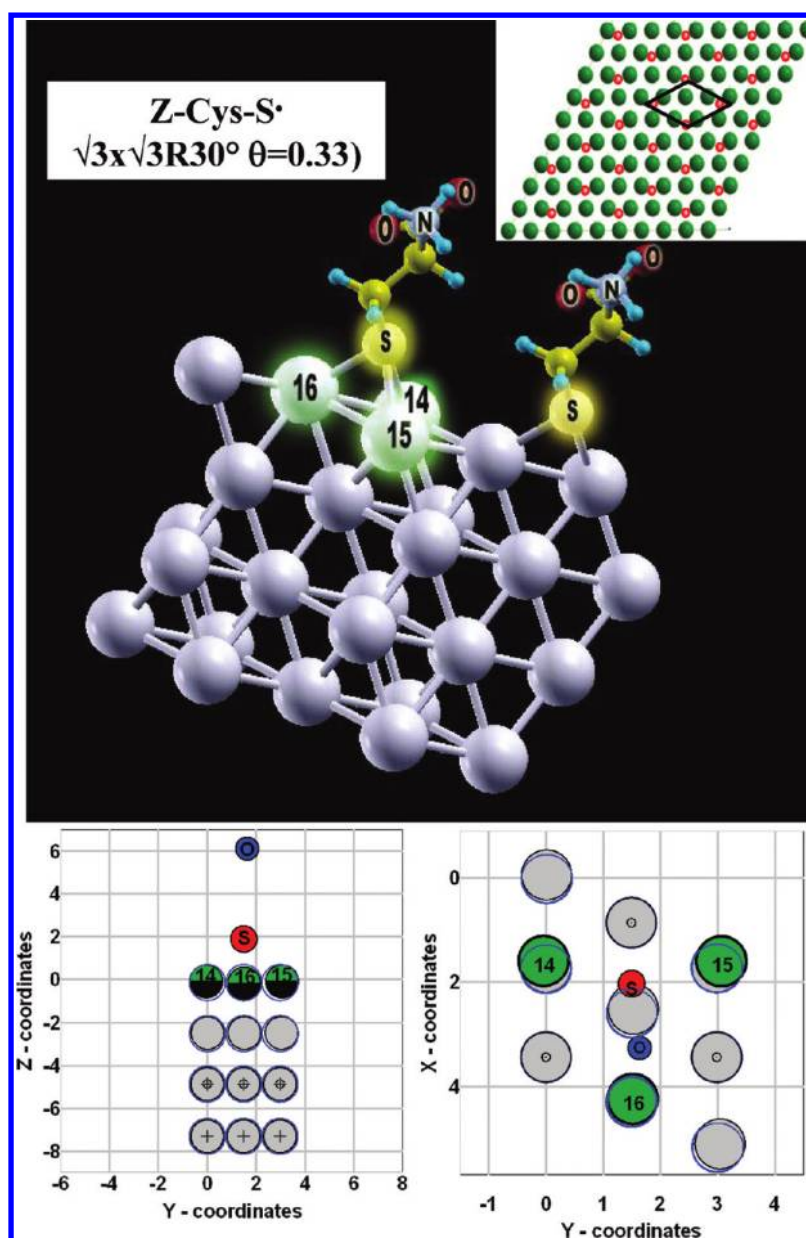


Figure 3. Top: 3D view of the relaxed system corresponding to Z-cys adsorbed at a bridge shifted toward hcp site ($\theta = 0.33$). The unit cell ($\sqrt{3} \times \sqrt{3}$) R 30° used for the calculations is also shown. Bottom: 2D side and top views of the structures. Green circles, upper Ag atoms; green-black circles, Ag atoms nearest to S (red filled circles) and O(6) (blue filled circles) atoms; gray circle, second layer of Ag atoms; gray circles with a central point, third layer of Ag atoms; gray circles with a central cross, fourth layer of Ag atoms. The size of the circles was not scaled with the real radius of the atoms, but their centers give their coordinates in Å. The blue circles around the Ag atoms represent their positions in the relaxed slab in absence of adsorbates.

weakening of the bond by the lateral interactions. The formation of zwitterionic species is only observed at the highest coverage of 0.33 (marked by a circle in Figure 1), indicating that probably the interaction between neighbors caused its formation. All these zwitterionic species are energetically more favorable by about 1 eV than the neutral radical.

We have selected two of these conformers, a neutral radical at low coverage and a zwitterionic species at high coverage (circles in the plot). Then we have relaxed these two species also in the x and y coordinates. The resulting structures were the L-cysteine radical L-cys ($\bullet\text{S}-\text{CH}_2-\text{CH}-\text{NH}_2-\text{COOH}$) adsorbed at a bridge site slightly displaced toward an fcc location, and the zwitterionic radical Z-cys ($\bullet\text{S}-\text{CH}_2-\text{CH}-$

$\text{NH}_3^+-\text{COO}^-$) adsorbed at a bridge site shifted to a hcp site within a (4×4) unit cell ($\theta = 0.06$) and a $(\sqrt{3} \times \sqrt{3})$ R 30° unit cell ($\theta = 0.33$), respectively.

Geometry and Energetics. Figure 2 shows the results for the relaxed geometry of adsorbed L-cysteine radical, and Figure 3 of the zwitterionic Z-cysteine radical on the Ag(111) surface at bridge sites. The values of the corresponding most relevant parameters are given in Table 1 in comparison with theoretical and experimental data from the literature. Table 2 shows the changes in the coordinates of the silver atoms interacting with the adsorbate. The relaxation of the slab previous to the adsorption shows a slight compression perpendicular to the surface of the two upper layers, as is usually observed with similar systems (in this case about 0.13 Å for the first layer and

Table 2. Perturbations of the Equilibrium Positions (in Å) of Silver Surface Atoms by the Presence of Adsorbed L-Cysteine Radical and Cysteine Zwitterionic Radical on Ag(111) Surfaces^a

silver atom	Δx	Δy	Δz	structure
Ag ₁₄	−0.139	−0.046	0.055	$\theta = 0.33$, Z-Cys-S [•] /Ag(111) ($\sqrt{3} \times \sqrt{3}$)
Ag ₁₅	−0.119	0.084	0.054	$\theta = 0.33$, Z-Cys-S [•] /Ag(111) ($\sqrt{3} \times \sqrt{3}$)
Ag ₁₆	−0.059	0.013	−0.046	$\theta = 0.33$, Z-Cys-S [•] /Ag(111) ($\sqrt{3} \times \sqrt{3}$)
Ag ₂₁	0.017	0.048	0.074	$\theta = 0.06$, LCysS [•] /Ag(111) (4×4)
Ag ₂₂	0.035	0.061	0.061	$\theta = 0.06$, LCysS [•] /Ag(111) (4×4)
Ag ₂₄	−0.031	−0.053	−0.022	$\theta = 0.06$, LCysS [•] /Ag(111) (4×4)
Ag ₂₆	−0.113	0.072	0.080	$\theta = 0.06$, LCysS [•] /Ag(111) (4×4)
Ag ₁₈	0.029	0.028	−0.028	$\theta = 0.06$, LCysS [•] /Ag(111) (4×4)
Ag ₂₅	−0.031	0.081	−0.021	$\theta = 0.06$, LCysS [•] /Ag(111) (4×4)

^aThe values are given relative to the prerelaxed slab without adsorbate. For distinguishing between the different atoms, see Figures 2 and 3.

about 0.08 Å for the second one). After adsorption, additional shifts on the coordinates of the silver atoms are observed,

mainly at the system with higher coverage. The silver atoms nearest to the adsorbate rearrange to form the bonds, showing the tendency to elongate their distances to the sulfur atom. However, these displacements are smaller than those observed on Au(111) and Au(110),^{19,20} where the adsorption of thiols produces a strong corrugation of the surface. The distance of the sulfur atom perpendicular to the surface is almost the same for both configurations (1.89 Å). The S atom is coordinated with two neighboring Ag atoms, labeled 22 and 26 for L-cys, and 14 and 15 for Z-cys, forming bonds with lengths of about 2.56 Å. They are slightly longer than the values calculated for cysteine and ethanethiol on Au(111) and Au(110).^{19,20} A weak interaction with the third Ag atom of the starting position of the hollow site (labeled 16 and 24 for L-cys and Z-cys, respectively) is still observed. The C_α–S–Ag angle remains practically unchanged from its starting value and coincides with that obtained for the adsorption of cysteine on Au(111). Also the different internal bond lengths remain similar to the free molecule in gas phase. Nevertheless, the C–S bond is lengthened by the interaction with the surface, indicating a weakening. A similar effect has been observed with cysteine adsorbed on Au(111)¹⁴ and on a silver cluster²³ (see Table 1). The distance between the oxygen atoms and the carbon for the carboxyl group also changes in the case of the Z-cys. It becomes about 1.28 Å for both oxygens due to the carboxyl deprotonation.

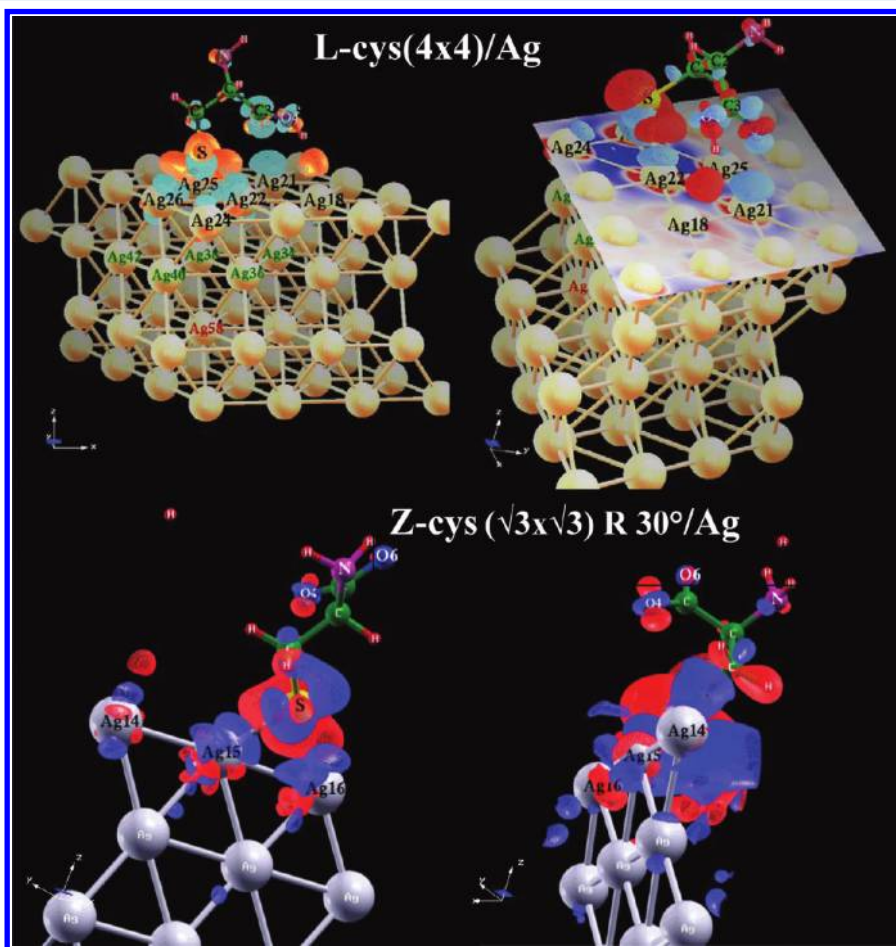


Figure 4. Isosurfaces of the charge density difference resulting from adsorption of the L-cys and Z-cys radicals on silver. Isovalue of $0.002 e/a_0^3$. The blue color represents the electron deficit regions, while the electron excess regions are colored in red-orange.

The most interesting features that we can distinguish between both configurations are related to the rearrangement of the functional groups (carboxyl and amine) in order to adjust themselves to the adsorption environment. The configuration at low coverage corresponding to the L-cys adsorbate has enough space available to rotate the carboxyl group, which now points toward the surface and interacts with it. One of the oxygen approaches up to a distance of 2.44 Å to the surface. The first neighbor O(6)–Ag(21) distance is 2.60 Å. Also the hydrogen of the carboxyl group is very close to the surface (2.29 Å). The first neighbor H(10)–Ag(18) distance is 2.58 Å. This indicates that also the carboxyl group participates in the bond with the surface, as we shall confirm later by analysis of the electronic structure. A similar situation has been observed for the amine group on Au(111).¹⁴

The formation of zwitterionic species is observed at highest coverage ($\theta = 0.33$). In this case, neighboring adsorbates have an optimal configuration such that the carboxyl and amine groups can interact and exchange a proton. As a consequence, the distance O₄–H appears longer than the one calculated for the other systems, and this hydrogen atom is now at a similar distance to the N atom as the other H atoms of the amine group (about 1.00 Å).

The torsion angles O₆–C₃–C₂–N, O_{4(H)}–C₃–C₂–N, and O₆–C₃–C₂–C₁ of the adsorbates strongly vary in comparison to the free molecule. On the contrary, the distortion of the C₃–C₂–C₁–S angle is minor, indicating that the backbone of the molecule remains almost intact under adsorption, while the rotation of the functional groups can be induced by interactions with the surface.

The energy values obtained for the adsorption of L-cys and Z-cys, regarding as starting species the isolated radicals relaxed within a large cell (7×7), are -2.67 and -3.06 eV, respectively. However, if the isolated L-cys and Z-cys radicals within their corresponding cells (i.e., (4×4) and $(\sqrt{3} \times \sqrt{3})$ R 30° , respectively) are considered as reference, such that lateral interactions are possible, the energy for the adsorption of L-cys at 0.06 coverage remains almost unchanged, but that for the adsorption of the zwitterionic radical becomes much less negative (-2.03 eV). These results indicate that there are practically no intermolecular interactions when the L-cys is adsorbed at low coverage, while in the case of the Z-cys the lateral interactions play an important role. Effectively, relaxation of the Z-cys species within the $(\sqrt{3} \times \sqrt{3})$ R 30° cell in the absence of surface produces only a small reorganization of the atoms, remaining in the zwitterionic configuration. If the more realistic picture is considered with the cysteine molecule as precursor and hydrogen molecule as side product, these values are still exothermic: -1.06 and -1.46 eV adding the difference to the first case, and -1.06 and -0.424 eV adding the difference to the second case. It is noticeable that although an increase of the adsorption energy is expected at higher coverage, the adsorption of Z-cys at 0.33 coverage appears more favorable than that of L-cys at 0.06 coverage when the relaxed Z-cys radical is selected as reference. It seems that the gain in energy by the formation of the zwitterionic species exceeds the steric effects between neighbors produced at higher coverage. It is also expected that in a solvent environment or in the presence of other ions this situation can still be improved by stabilization of these species.^{17,18}

Electronic Properties: Charge Density Difference Resulting upon Adsorption. First, we analyze the electronic structure, focusing on the electronic density differences of the

system produced by the adsorption. Figure 4 shows isosurfaces of the charge density difference resulting from adsorption of both investigated species, the L-cys (Figure 4, top) and the Z-cys (Figure 4, bottom) radicals on Ag(111). Figures including more details are available in the Supporting Information. The complexity of the bonds is evident.

We can clearly observe regions of electronic charge accumulation (red) and regions of depletion (blue). The increased accumulation of charge between the sulfur atom and the surface is an indication of the enhanced chemical bonding with sigma-character. However, the charge distribution reveals a complicated interplay of the different atomic orbitals involved in the bond. In the case of the tilted L-cys radical adsorbed at low coverage, one notices the redistribution of charge in the carboxyl group indicating that this group is also participating in the bond with the surface. There is a considerable increase of electronic charge between the hydrogen of the hydroxyl group H(10)O(4) and the silver atom denoted as Ag18, indicating the tendency to form a bond with σ -character. On the contrary, between the oxygen of the carboxyl labeled as "O6" and the silver atom Ag21, a significant decrease of the electronic density is observed, indicating repulsion. Slight changes are also depicted in the carbon bonded to the sulfur atom and the nitrogen of the amine group.

To aid the interpretation, we plotted electron density contours projected onto various planes through the bonds between atoms. Figure 5 shows the contour plots for the top

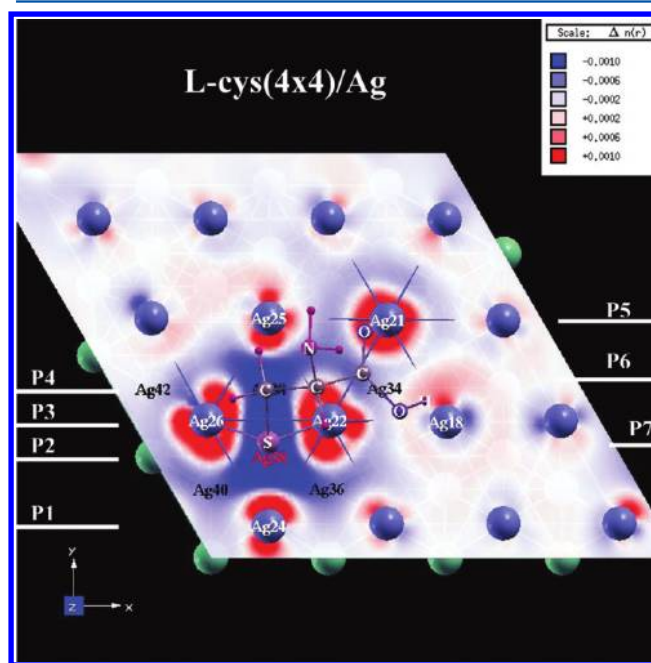


Figure 5. Cross section of the charge density difference at the silver surface ($z = 0$) drawn in linear scale from -0.001 to 0.001 e/a_0^3 with an increment of 0.001 e/a_0^3 . The silver atoms of the top layer close to the adsorbate are labeled in white (Ag22, Ag24, Ag26, Ag21, Ag18, Ag25). The silver atoms of the second layer are labeled in black (Ag42, Ag38, Ag34, Ag40, Ag36). The silver atom of the third layer just below the sulfur atom is labeled in red (Ag58). Electronic charge flows from blue to red regions. The orientation of perpendicular planes, whose charge differences are shown in Figure 6, are also drawn (P1→P7).

layer of silver when the L-cys radical is adsorbed at a coverage of 0.06. The silver atoms closest to the sulfur atom which forms the bonds (Ag26 and Ag22) as well as that closest to the

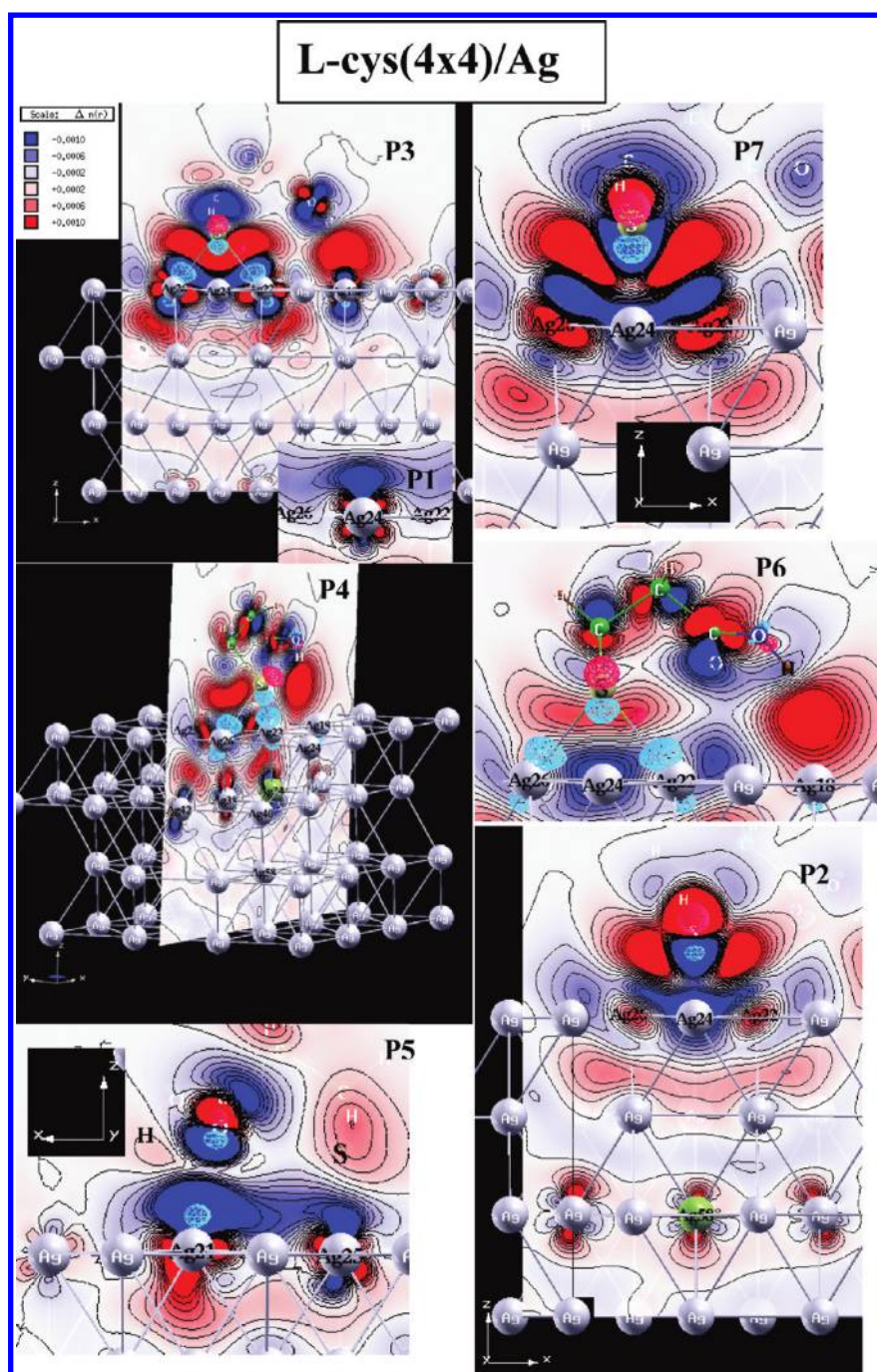


Figure 6. Cross section of the charge density difference at various planes ($z-x$) perpendicular to the silver surface ($z = 0$) and to the axis y , drawn in linear scale from -0.001 to 0.001 e/a_0^3 with the increment of 0.001 e/a_0^3 . The plane P3 crosses the silver atoms of the top layer, Ag22, Ag26, and Ag18; the plane P7 crosses the sulfur atom; the plane P1 crosses the silver atom of the top layer Ag24; the plane P4 crosses the silver atoms of the second layer, Ag42, Ag38, and Ag34; the plane P6 crosses the carbon chain; the plane P5 crosses the silver atoms of the top layer, Ag21 and Ag25; the plane P2 crosses the silver atom Ag58 of the third layer. The orientation of these planes is shown in Figure 5.

oxygen O6 of the carboxyl group (Ag21) are slightly up-shifted (see also geometrical parameters in Table 2).

In this plane, an appreciable increase of the electronic charge around the silver atoms interacting with the adsorbate (Ag22, Ag26, Ag21, Ag24, Ag25, Ag18) is observed, while in the regions directly below the sulfur atom a strong depletion of the charge occurs.

Figure 6 shows various cross sections of the charge density difference through diverse bonds for this system. Figures including more details are available in the Supporting

Information. The plane P3 crosses the silver atoms of the silver top layer: Ag22, Ag26, and Ag18. The electronic flow from atomic orbitals of Ag22, Ag26 to the region below the sulfur atom and from the Ag18 to the region below the hydrogen atom of the hydroxyl group is clearly observed, evidencing the formation of σ bonding states. The third silver atom (Ag24) participating in the bond with the sulfur also shows charge redistribution (see also contour on P1), but the interaction is weaker than that of the other two atoms (Ag22 and Ag26). The cross section through the sulfur atom (see P7)

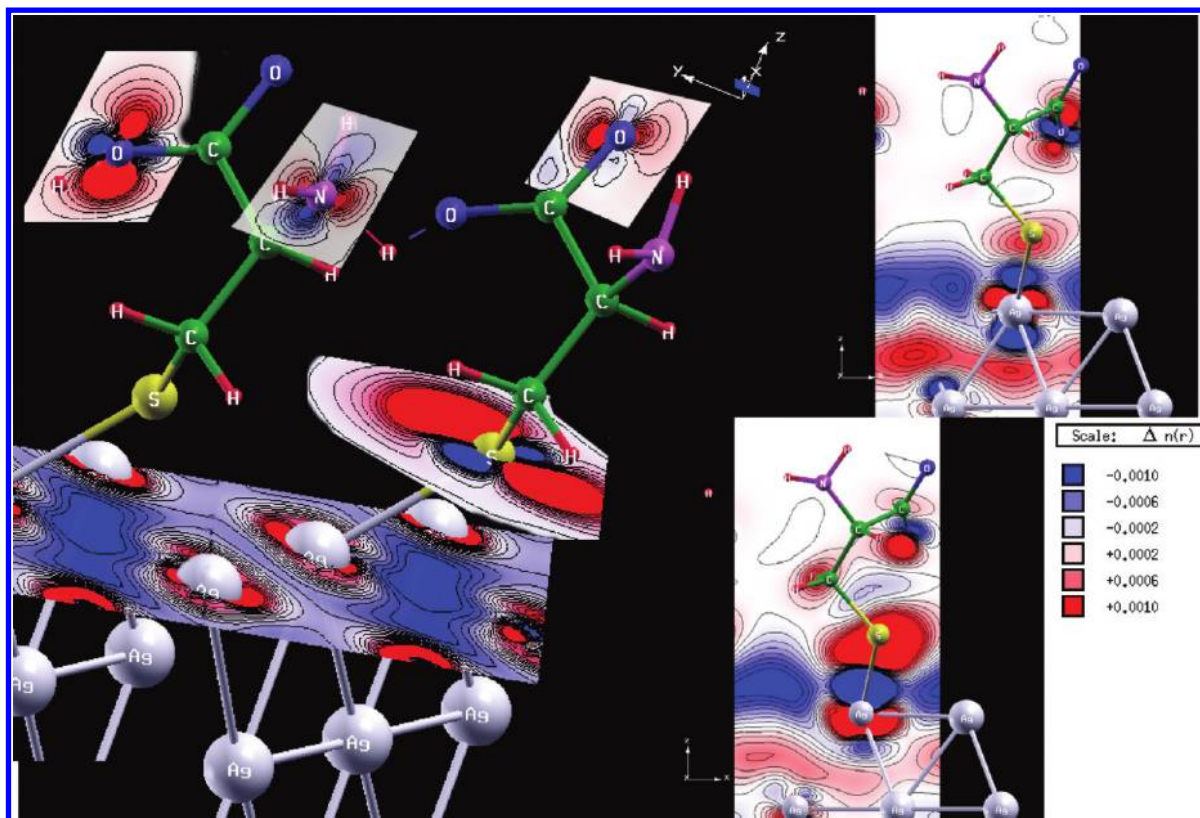


Figure 7. Cross-section of the charge density difference for Z-cys radicals on silver at several planes drawn in linear scale from -0.001 to $0.001 e/a_0^3$ with an increment of $0.001 e/a_0^3$.

displays a depletion of electronic charge in the intermediate region, which could be interpreted as a π -antibonding orbital. However, this interpretation must be taken with care, since these plots correspond to TOTAL electronic density difference; an analysis of integrated local density of states (ILDOS) is required. The redistribution of charge occurs not only at the top layer of silver, but also at the second and third one, as evident from the contours shown in P4 (cross section through Ag42, Ag38, Ag34) and in P2 (the line containing the atom Ag58 and their two neighbors). The alkyl chain is also affected, as can be observed in P6. The repulsion between the oxygen labeled as O6 and the surface atoms Ag21 and Ag25 can be clearly distinguished on the contour of P5.

Figure 7 shows cross sections for the charge density difference in the case of the Z-cys radical adsorbed on Ag(111) at a 0.33 coverage (unit cell $(\sqrt{3} \times \sqrt{3}) R 30^\circ$). The interaction of the sulfur atom with the surface atoms is similar as for the L-cys radical at low coverage. However, neither the carboxyl nor the amine group strongly interact with the substrate due to the upright position of the adsorbate. Here one notices an increase of electronic charge on both oxygens of the carboxyl group and a simultaneous decrease on the nitrogen atom of the amine group due to the zwitterionic character of this adsorbate.

Electronic Properties: Density of Electronic States Projected onto the Different Atoms. We have also performed a detailed analysis of the density of electronic states projected onto different atomic orbitals (PDOS) for both conformations of the adsorbed species, L-cys and Z-cys.

As discussed in the last section, the interaction of the metal is particularly strong with the states of the sulfur atom, which is nearest to the silver surface.

Figure 8 shows the PDOS onto the sulfur atom (red lines) and onto the α -carbon atom (shaded green pattern) bonded to it (labeled in Table 1 as S and C1, respectively) in the case of the free radicals (L-Cys and Z-Cys) fixed at the configurations when they are adsorbed, but in the absence of the substrate (first and second plot at top), and when they are adsorbed on Ag(111) forming a L-cys- (4×4) and Z-cys- $(\sqrt{3} \times \sqrt{3}) R 30^\circ$ structures (plots at bottom). The vertical lines indicate the position of the Fermi level (E_F), which is taken from the self-consistent calculations. In the noninteracting case, these lines separate the highest occupied molecular orbitals (HOMO) from the lowest unoccupied molecular orbitals (LUMO). Because the Fermi level characterizes the energy up to which the states in the metal slab are filled, the energy differences between E_F and the HOMO and the LUMO correspond to the hole- and electron-injection barriers into the adsorbed layer.^{32,33} Thus, the effect of the interaction with the metal on the electronic structure can be easily inferred by comparison of the systems.

The overlap between electronic states corresponding to the carbon and to the sulfur atoms indicates the participation of such states in the formation of molecular bonds between both atoms. However, due to the hybridization and the interaction with the metal, the assignment of PDOS features to individual molecular orbitals is not always straightforward. First, we analyze the results for the free radicals. Two distinct features are obtained for both spins, with occupation numbers for the L-Cys radical of 0.92 and 0.65 for up and down spins, respectively, and for the Z-Cys radical of 0.84 and 0.65, respectively. In the region between -8 and -3 eV, a series of peaks due to the hybridization between s and p states is observed. There is a partial lower overlap between the states corresponding to the

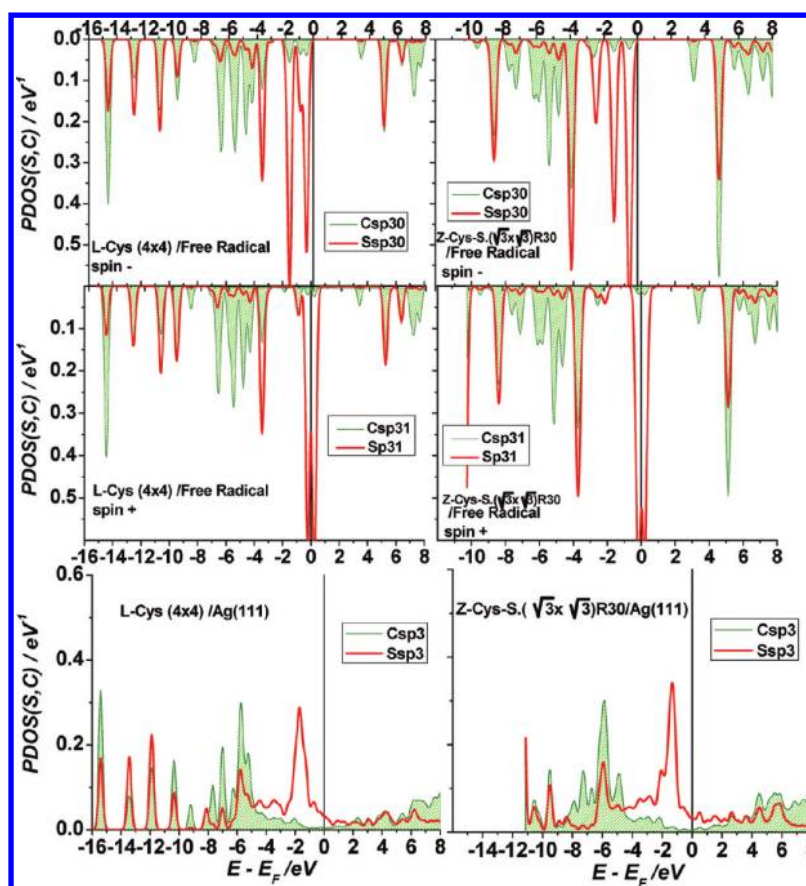


Figure 8. Density of states for the systems: L-cys-free radical (left) (top, spin+ and second plot, spin−), L-cys-(4 × 4)/Ag(111) (third plot), and Z-cys-($\sqrt{3} \times \sqrt{3}$) R 30° free radical (right, top, spin+ and second plot, spin−), Z-cys-($\sqrt{3} \times \sqrt{3}$) R 30°/Ag(111) = (bottom, right) projected onto the sulfur atom (red lines) and onto the α -carbon bonded to it. In the case of the free radicals, both spin orientations were considered. The vertical line indicates the position of the Fermi level.

carbon and sulfur atoms for the peaks in the region of $-8 \rightarrow -5$ eV, with a larger contribution of the carbon atom, while the overlap corresponding to the sharp peak at -3.8 eV has a larger contribution from the sulfur atom. At about $+5$ eV, a sharp overlap peak is observed between the sulfur and carbon atoms, which can be attributed to antibonding states between both. The L-cys radical displays also a second smaller overlap peak at about $+6.5$ eV. Near the Fermi level, the sulfur shows electronic states indicating a small overlap with states of the carbon, which correspond to the unpaired electron of the radicals and the unshared pairs of electrons. Therefore, these states are in condition to interact with the electronic states of the metal to form Ag–S bonds. For both conformers (L-cys and Z-cys), the features of the states in this region are almost similar and are sensitive to the spin polarization.

In the case of the species adsorbed at the silver surface, the results for both spins are identical as expected. The occupation numbers of the sulfur states are in this case 0.82 for the L-cys-(4 × 4) structure and 0.75 for the Z-cys-($\sqrt{3} \times \sqrt{3}$) R 30° structure. The strong localized states below -8 eV are less affected by the presence of the metal and only downshifted to lower energies when the L-Cys species are adsorbed on the metal.

In the region above -8 eV, due to the presence of sp- and d-bands of the substrate, the electronic states of the adsorbed species are not only shifted but also substantially broadened as a consequence of a strong coupling with the electronic states of the metal. The peaks at -5.8 and -1.7 eV are usually attributed

to bonding and antibonding states with the metal resulting from the split of electronic states of sulfur around the d-band.^{13,14} However, it is clear from this picture that no split takes place before the adsorption. They correspond to hybridization of the atomic orbitals of sulfur and carbon before the adsorption (compare with the PDOS obtained for the free radicals analyzed above). Here, we notice that the bonding states between sulfur and carbon atom (around -5.8 eV) are simply also affected and broadened. If there is an antibonding state between sulfur and the surface in this region, it is overlapped and cannot be distinguished from the bonding states between carbon and sulfur.

In accord with the results of the charge differences shown in the previous section, not only does the sulfur atom interact with the silver surface, but also the carboxyl group plays an important role in the formation of bonds, especially in the case of the tilted adsorbed L-cys radical at low coverage. Figure 9 shows the density of states projected onto the atoms of the carboxyl and amine groups. Similar to the case of the sulfur atom, we can also distinguish an overlap between electronic states of the oxygen atoms and electronic states of the carbon atom corresponding to the carboxyl group (labeled in Table 1 as O6, O4, and C3, respectively). In the case of the isolated system, the overlap of the sharp peaks below -4 eV can be attributed to bonding states, while those at about $+3.5$ eV to antibonding states between the O6, O4, and C3 atoms. Coincident sharp peaks for the hydrogen (H12) and the

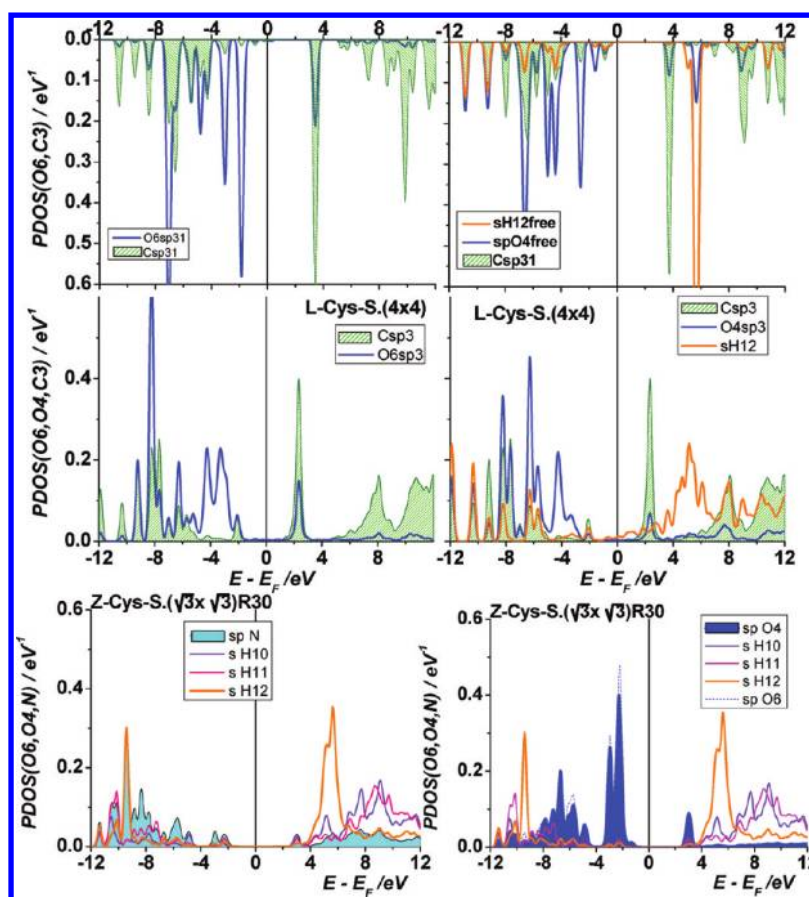


Figure 9. Density of states for the systems: L-cys-free radical (top), L-cys-(4 × 4)/Ag(111) (center), and Z-cys-($\sqrt{3} \times \sqrt{3}$) R 30° (bottom) projected onto both oxygen atoms of the carboxyl (O4 and O6 (blue lines)), onto the carbon of the carboxyl (green lines), onto the nitrogen of the amine group (cyan shadow), onto the hydrogen atoms of the amine group H10, H11 (violet and pink lines), and onto the hydrogen atom H12 of the carboxyl bonded to the oxygen O4 before adsorption. The vertical line indicates the position of the Fermi level.

oxygen (O4) of the carboxyl group appearing at +5.5 eV represent antibonding states between both atoms. The two peaks observed at −3.0 and −1.8 eV for the O6 of the noninteracting system can be assigned to the lone electron pairs, since they do not show any overlap with other atoms of the molecule. Therefore, they are suitable to interact with the metal. Effectively, a shift of about 1.5 eV to lower energies and a broadening is observed for these electronic states of the oxygen atom O6 when the species is adsorbed on the surface. In the case of O4, these states appeared at more positive energies, and they also overlap with the electronic states of the 1s orbital of the hydrogen atom (labeled as H12) bonded to this oxygen atom. The small peak appearing at −2 eV in the PDOS onto O4 and O6 overlaps with states of the H12 and C3 in the case of O4, while in the case of O6 only with C3 states. Nevertheless, the electronic states in the energy range of the metal bands of both oxygen atoms of the carboxyl group, which is near to the surface for the tilted L-cys configuration, become broader, as can be observed from Figure 9. Also the antibonding states between the O4 and the H12 are strongly affected. The contribution corresponding to the O4 is absent and that of the H12 is broadened, indicating the weakness of the bond O4–H12 and a strong interaction of H12 with the substrate. This result is in concordance with the increase of charge observed between H12 and Ag18 (see previous section, Figures 4 and 6).

All these facts clearly indicate that, for this geometric configuration, the bond between the L-cys radical and the silver surface mainly occurs through the sulfur atom with additional important contributions of the carboxyl group. Similar effects have been observed by Di Felice et al.¹⁴ and by Höflling et al.,¹⁹ when the neutral radical is adsorbed on Au(111) and on Au(110), with the amine group pointing to the surface, respectively. In our case, the amine group is pointing away from the substrate, and therefore, the interaction with the metal is weak. However, an orientation of the amine group to the surface should also be possible. As we have mentioned in the Introduction, the three functional groups are able to interact with the metal surface, and the relative conformational energies are within a few meV. We have chosen a particular one as an example.

In the case of the adsorbed zwitterionic species Z-Cys, interesting changes occur in the features corresponding to the hydrogen atom labeled H12. For this configuration, this atom forms a bond with the nitrogen of the amine group instead of a bond with the O4 of the carboxyl group. Thus, their states overlap with those of the nitrogen, and both oxygen atoms (O6 and O4) show the same distribution of electronic states with a very weak overlap with the H12. The electronic states corresponding to the other two hydrogen atoms of the amine group (H10 and H11) are a little different from those of H12. However, the geometrical configuration is also different for

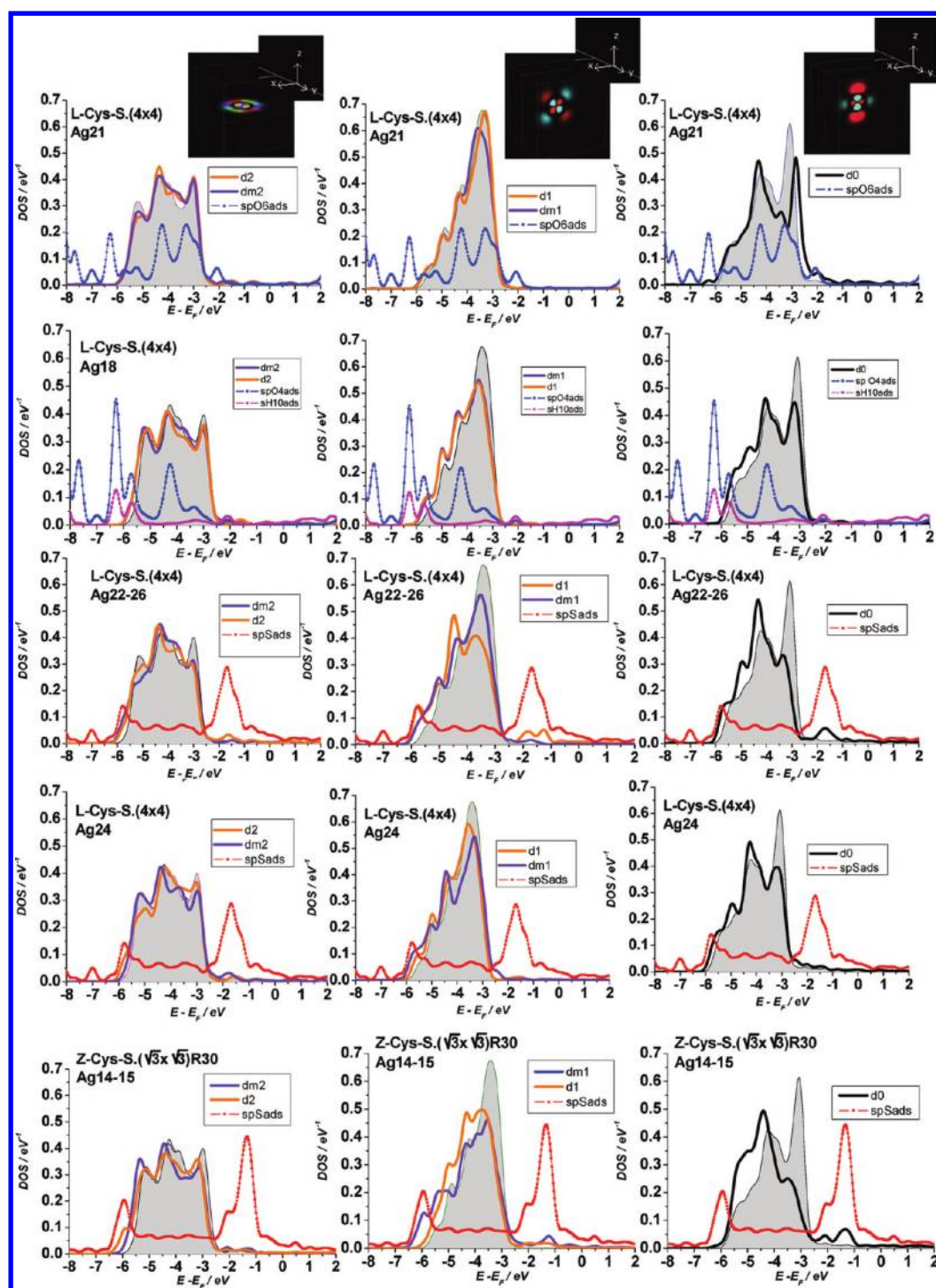


Figure 10. Components of the density of states of the d-bands projected onto the surface silver atoms interacting more strongly with both adsorbates, L-cys and Z-cys. (The levels of the atoms are given for each plot.) The sp³ states of oxygen atoms (O6 and O4) and of the sulfur atoms are also shown.

these atoms and the intramolecular interaction with other atoms of the Z-Cys species can induce these differences.

These are examples of the variety of ways for the adsorption of cysteine. The intramolecular interactions and conformational lability of this amino acid due to the existence of different functional groups, leads to more than one preferred mode of interaction with the substrate.

In order to investigate the electronic coupling with the substrate, we have also analyzed in detail the modification on

the electronic states corresponding to selected atoms of the metal. A detailed analysis of the electronic density of states has been previously performed by Höfiling et al.¹⁹ for single cysteine adsorption on Au(110). These authors have found that the states projected onto the gold surfaces were only marginally affected by the single-molecule adsorption. However, the projection of states had been carried out onto the whole substrate. Thus, local effects on particular atoms of the surface interacting with the adsorbed species do not show. From the

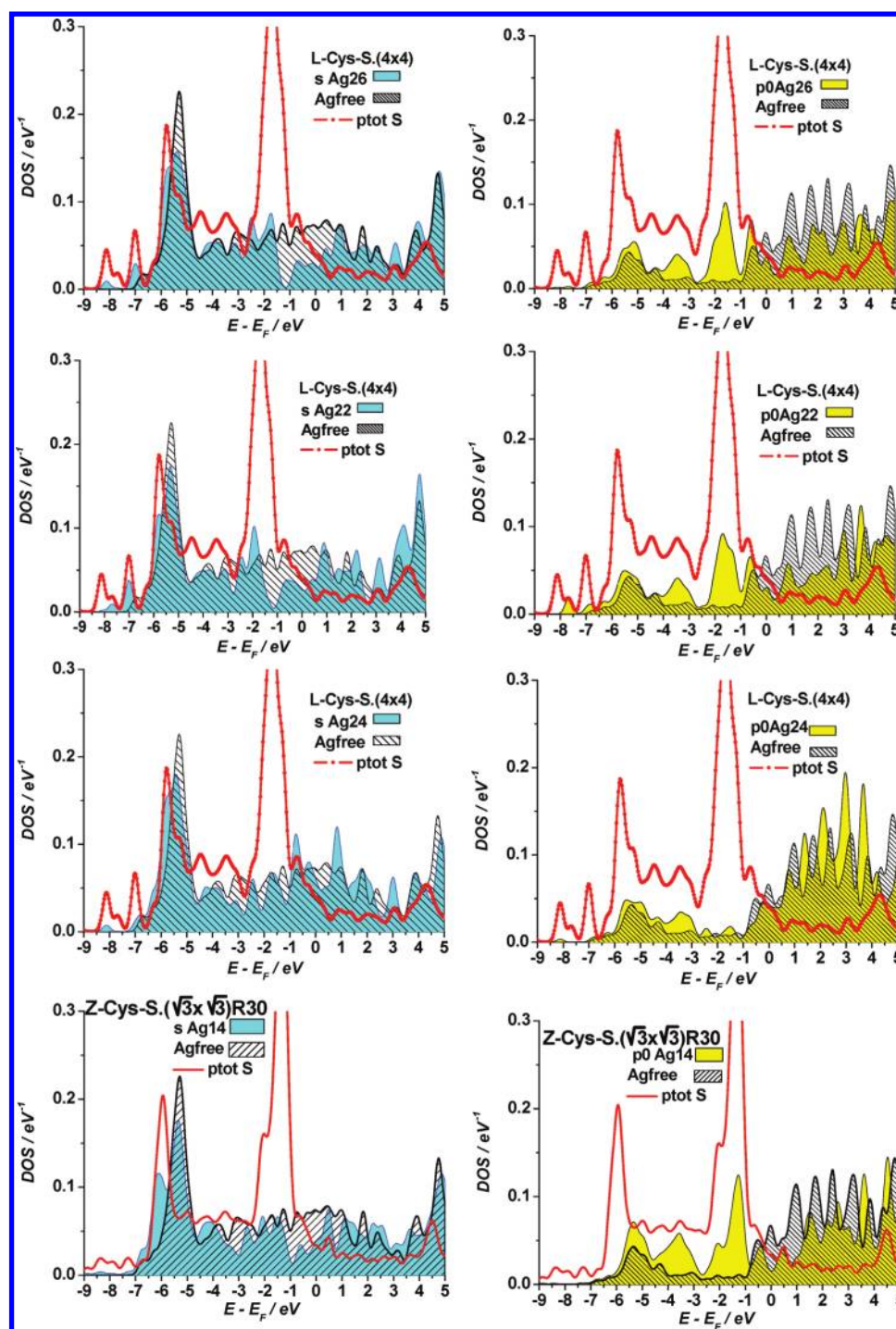


Figure 11. Components of the density of states of the s- and p-bands projected onto the surface silver atoms interacting more strongly with both adsorbates, L-cys and Z-cys. (The levels of the atoms are given for each plot.) The sp3 states of the sulfur atoms are also shown.

results of charge differences contours shown in the previous section, it is evident that the electronic states of some of the silver atoms are more affected than others. In order to investigate the electronic coupling with the substrate, we have also analyzed in detail the modification on the electronic states of the metal, but we have focused on selected atoms of silver. We have followed the same strategy as in our previous work^{20,34} about the adsorption of ethanethiol on Au(111) and about the adsorption of OH on Pt(111).

Figure 10 shows the projection of the components of the d-bands onto the silver atoms nearest to the adsorbate. The

atoms are labeled as in Figures 2 and 3 (see also Table 1). The sulfur states are also included for comparison. According to the spatial distribution of the orbitals and their symmetry properties, three distinguishable features are observed for a bare surface of Ag. The presence of an adsorbate interacting with the metal breaks the symmetry of the metal orbitals, and five different features are obtained. A redistribution of the electronic states takes place, the states with a larger extension in the direction perpendicular to the surface being most affected. The center of the d-bands is defined as³⁵

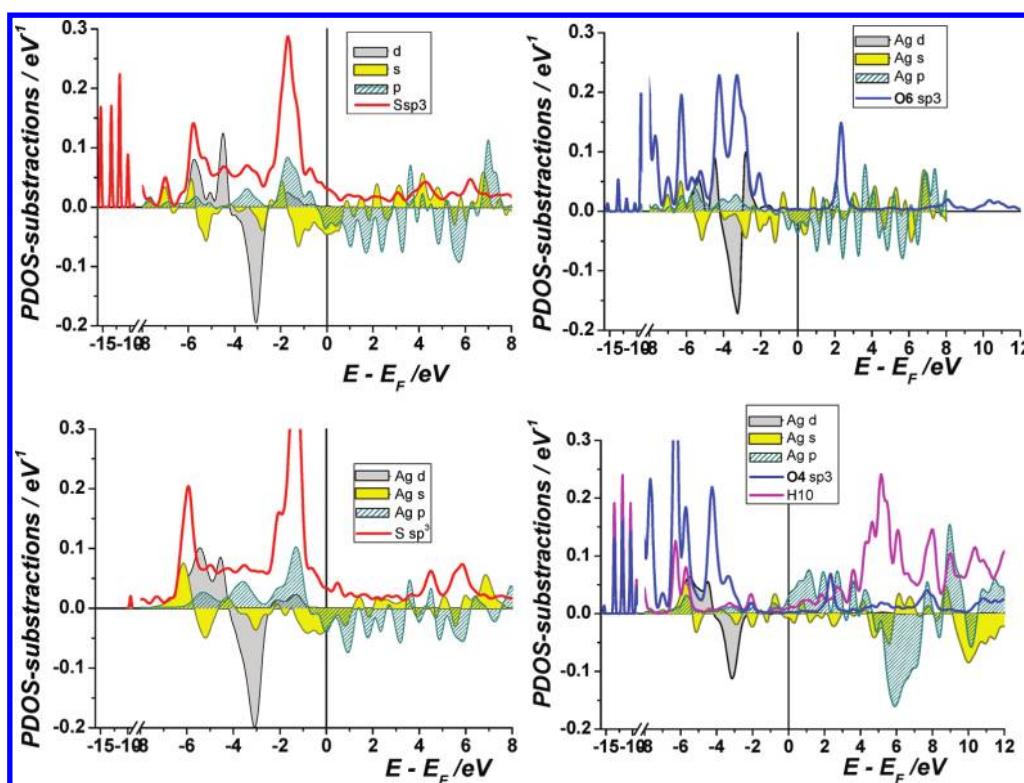


Figure 12. Differences between the projected density of states of a silver surface atom in the absence and the presence of an adsorbed species. (dashed surfaces). (The levels of the atoms are given for each plot.) The sp³ states of the sulfur atom, the oxygen atoms O6 and O4, and the hydrogen atom H10 are also shown.

$$\frac{\int_{-\infty}^{+\infty} E\rho(E) dE}{\int_{-\infty}^{+\infty} \rho(E) dE}$$

and is shifted to lower energies upon adsorption: -0.10 eV ($d_{\pm 2}$), -0.18 eV ($d_{\pm 1}$), and -0.21 eV (d_0) for the silver atoms at the bridge position (Ag22–26) when L-cys is adsorbed. This effect is stronger when Z-cys is adsorbed. These values for this system are -0.21 eV ($d_{\pm 2}$), -0.20 eV ($d_{\pm 1}$), -0.24 eV ($d_{\pm 1}$), and -0.25 eV (d_0) for the silver atoms at the bridge position (Ag14–15). In these two cases, new states appear between -2.0 and -1.0 eV. These states are coincident with electronic states of the sulfur atom corresponding to the asymmetric peak at -1.7 eV. An important depletion is observed at around -3.0 eV, and also a slight increase at the left side of the bands around -5.0 eV is evident. The silver atoms interacting with the carboxyl group also show changes, although less noticeable. In the case of Ag21, the d-band practically does not shift its center. The feature of the d_0 states is affected around -3 eV. The silver atom Ag18, which interacts with the OH of the carboxyl group, shows a larger shift in the center of the d-band than Ag21: -0.12 eV ($d_{\pm 2}$), -0.18 eV ($d_{\pm 1}$), and -0.22 eV (d_0).

Usually, less attention is paid to the sp bands of the metal, although they also play an important role in the adsorption process, as we shall demonstrate next. Figure 11 shows the changes produced in the s and p bands projected onto the silver atoms nearest the adsorbate. The sulfur states are also included for comparison. At -5.8 eV, the s states of the silver atoms nearest to the adsorbate (Ag21,22,24,26) show a peak, which was absent for the bare surface. This coincides with the peak where an overlap occurs between states of the sulfur atom and the carbon atom C1 bonded to it. Simultaneously, a depletion

on the density of states of the peak at -5.3 eV is observed. New small peaks appear immediately below the left border of the s-band, which overlap with electronic states of the adsorbate (located on both carbon C1 and sulfur atoms). A similar effect is observed with the silver atom (Ag21) nearest to the oxygen atom O6 (see plot in the Supporting Information). Depletion of the density of states of the s-band can be observed around the Fermi level (between -1.5 and $+1.0$ eV for Ag 22–26, and between -3.0 and $+1.0$ eV for Ag21). The p states of the silver atoms nearest to the sulfur atom (Ag22–26) show two main new peaks at around -3.5 eV and around -1.7 eV, whose features almost coincide with those peaks of the sulfur states. The corresponding states of the Ag24 show only the peak at -3.5 eV. Similar situation is observed on the p states projected onto the silver atom (Ag21) nearest to the oxygen atom O6. A double peak appears at -4.2 and -3.2 eV coincident with electronic states of the oxygen. In this case, also a series of small peaks just below the left border of the p-band are observed. In the case of the silver atom 18 near the O4 and H10 atoms, no appreciable changes are observed below the Fermi level. However, at energies above 3 eV, some changes are evident.

In order to understand better the interplay between the different electronic states of the system, in Figure 12 we have plotted the difference of the electronic density between selected orbitals of interacting system and its isolated constituents (L-cys radical, Z-cys radical, and bare surface). This figure distinctly reveals the complicated feature of the adsorption. Although the total occupation of the electronic states of the metal does not change, a redistribution of them occurs between the different bands. It is noticeable that the occupation of p states increases for the atoms interacting with the sulfur atom, while that of the s states decreases, compensating each other. The energy regions

where the increase in the population of p states occurs, coincides with the position of peaks in the density of states of the sulfur atom. The p states of Ag18 show an important decrease of the unoccupied density of states at about +6 eV coincident with the broad peak of the H12. Apparently, there is a drift of electrons not only within each band, but also an electronic flow between different bands. The occupation of the d-bands displays redistribution in the energy range, but the changes vanish below the Fermi level. These effects are observed for both the silver atoms near the sulfur atom (Ag22–26) and those positioned near the oxygen atoms (Ag21 and Ag18). The d-bands show an increase in their populations below the center of the band ($E_c \approx -4$ eV) and a decrease above it. The occupation of the electronic states corresponding to the sulfur atom slightly increases upon adsorption. However, this number (0.17 e^-) should be taken with care, since it is within the calculation errors of DFT. The occupation of the electronic states corresponding to the oxygen atom changes less than 1%. Then, we can conclude that the formation of bonds between the adsorbate and the metal involves the simultaneous participation of different orbitals given a complicated hybridization feature.

On the technical side, we have still to mention an issue to be discussed: DFT does not properly describe dispersion forces. This will cause errors in close packing of the adsorbates, and we are aware of this shortcoming. However, L-cysteine is a short chain alkylthiol (C3) which strongly interacts with the metal surface mainly through the thiol group and less strongly through the carboxyl and amine groups. van der Waals forces are expected to be negligible in comparison with the electrostatic and chemical forces between these groups and the surface. The effect of dispersion forces can be considerable in the case of noncovalent mechanism of peptide adsorption as pointed out by Heinz et al.,³⁷ where a “soft epitaxy” mechanism of binding has been suggested.

CONCLUSIONS

We have investigated the geometry, energetic, and electronic properties of L-cysteine adsorption on Ag(111), not only qualitatively but also quantitatively. An exhaustive analysis has been performed using DFT calculations. The adsorption energy increases with coverage. At low coverage, a flat configuration exists where not only the sulfur atom but also the carboxyl group strongly interacts with the surface. Zwitterionic species have been found to be more favorable at higher coverages. It is noticeable that silver atoms in the second and third layer below the surface show changes in their electronic distribution. The formation of bonds between the adsorbate and the metal involves the simultaneous participation of different orbitals given a complicated hybridization feature. Bonds with σ and π character are formed. Also the electronic states of the α carbon atom participating in the bond with the sulfur atom are affected.

ASSOCIATED CONTENT

Supporting Information

Additional figures. This material is available free of charge via the Internet at <http://pubs.acs.org>.

AUTHOR INFORMATION

Corresponding Author

*E-mail: esantos@uni-ulm.de.

Notes

The authors declare no competing financial interest.

ACKNOWLEDGMENTS

We thank Wolfgang Schmickler for discussions and Paola Quaino and Martin Zoloff Michoff for helping to calculate the isosurfaces. Financial support by the Deutsche Forschungsgemeinschaft (FOR1376) of the European Union under FP7-People-2007-1-1 (ELCAT, Grant Agreement No. 214936-2) and by an exchange agreement between the DAAD and MinCyT is gratefully acknowledged. E.S. thanks CONICET (PIP 112-201001-00411) for continued support.

REFERENCES

- (1) Gronert, S.; O'Hair, R. A. J. *Ab Initio Studies of Amino Acid Conformations. 1. The Conformers of Alanine, Serine, and Cysteine*. *J. Am. Chem. Soc.* **1995**, *117*, 2071–2081.
- (2) Maul, R.; Ortmann, F.; Preuss, M.; Hannewald, K.; Bechstedt, F. DFT studies using supercells and projector-augmented waves for structure, energetics, and dynamics of glycine, alanine, and cysteine. *J. Comput. Chem.* **2007**, *28*, 1817–1833.
- (3) Fernández-Ramos, A.; Cabaleiro-Lago, E.; Hermida-Ramón, J. M.; Martínez-Núñez, E.; Peña-Gallego, A. DFT conformational study of cysteine in gas phase and aqueous solution. *THEOCHEM* **2000**, *498*, 191–200.
- (4) Tarakeshwar, P.; Manogaran, S. Conformational effects on vibrational frequencies of cysteine and serine: an ab initio study. *THEOCHEM* **1994**, *305*, 205–224.
- (5) Tarakeshwar, P.; Manogaran, S. Vibrational frequencies of cysteine and serine zwitterions – an ab initio assignment. *Spectrochim. Acta, Part A* **1995**, *51*, 925–928.
- (6) Tiwari, S.; Mishra, P. C. Vibrational spectra of cysteine zwitterion and mechanism of its formation: Bulk and specific solvent effects and geometry optimization in aqueous media. *Spectrochim. Acta, Part A* **2009**, *73*, 719–729.
- (7) Dakkouri, A. S.; Kolb, D. M.; Edelstein-Shima, R.; Mandler, D. Scanning Tunneling Microscopy Study of L-Cysteine on Au(111). *Langmuir* **1996**, *12*, 2849–2852.
- (8) Zhang, J.; Chi, Q.; Nielsen, J. U.; Friis, E. P.; Andersen, J. E. T.; Ulstrup, J. Two-Dimensional Cysteine and Cystine Cluster Networks on Au(111) Disclosed by Voltammetry and in Situ Scanning Tunneling Microscopy. *Langmuir* **2000**, *16*, 7229–7237.
- (9) Brolo, A. G.; Germain, P.; Hager, G. Investigation of the Adsorption of L-Cysteine on a Polycrystalline Silver Electrode by Surface-Enhanced Raman Scattering (SERS) and Surface-Enhanced Second Harmonic Generation (SESHG). *J. Phys. Chem. B* **2002**, *106*, 5982–5987.
- (10) Hager, G.; Brolo, A. G. Adsorption/desorption behaviour of cysteine and cystine in neutral and basic media: electrochemical evidence for differing thiol and disulfide adsorption to a Au(111) single crystal electrode. *J. Electroanal. Chem.* **2003**, *550–551*, 291–301.
- (11) Hager, G.; Brolo, A. G. Protonation and deprotonation of cysteine monolayers probed by impedance spectroscopy. *J. Electroanal. Chem.* **2009**, *625*, 109–116.
- (12) Shin, T.; Kim, K.-N.; Lee, C.-W.; Shin, K. S.; Kang, H. Self-Assembled Monolayer of L-Cysteine on Au(111): Hydrogen Exchange between Zwitterionic L-Cysteine and Physisorbed Water. *J. Phys. Chem. B* **2003**, *107*, 11674–11681.
- (13) Di Felice, R.; Selloni, A.; Molinari, E. DFT Study of Cysteine Adsorption on Au(111). *J. Phys. Chem. B* **2003**, *107*, 1151–1156.
- (14) Di Felice, R.; Selloni, A. Adsorption modes of cysteine on Au(111): Thiolate, amino-thiolate, disulfide. *J. Chem. Phys.* **2003**, *120*, 4906–4914.
- (15) Kühnle, A.; Linderth, T. R.; Hammer, B.; Besenbacher, F. Chiral recognition in dimerization of adsorbed cysteine observed by scanning tunneling microscopy. *Nature* **2002**, *15*, 891–893.

- (16) Šljivančanin, Ž.; Gothelf, K. V.; Hammer, B. Density Functional Theory Study of Enantiospecific Adsorption at Chiral Surfaces. *J. Am. Chem. Soc.* **2002**, *124*, 14789–4794.
- (17) Nazmutdinov, R. R.; Zhang, J.; Zinkicheva, T. T.; Manyurov, I. R.; Ulstrup, J. Adsorption and In Situ Scanning Tunneling Microscopy of Cysteine on Au(111): Structure, Energy, and tunneling Contrasts. *Langmuir* **2006**, *22*, 7556–7567.
- (18) Nazmutdinov, R. R.; Manyurov, I. R.; Zinkicheva, T. T.; Jang, J.; Ulstrup, J. Cysteine adsorption on the Au(111) surface and the electron transfer in configuration of a scanning tunneling microscope: A quantum-chemical approach. *Russ. J. Electrochem.* **2007**, *43*, 328–341.
- (19) Höfiling, B.; Ortmann, F.; Hannewald, K.; Bechstedt, F. Single cysteine adsorption on Au(110): A first-principles study. *Phys. Rev. B* **2010**, *81*, 0454071–04540712.
- (20) Tielens, F.; Santos, E. AuS and SH Bond Formation/Breaking during the Formation of Alkanethiol SAMs on Au(111): A Theoretical Study. *J. Phys. Chem. C* **2010**, *114*, 9444–9452.
- (21) Santos, E.; Lundin, A.; Pötting, K.; Quaino, P.; Schmickler, W. Model for the electrocatalysis of hydrogen evolution. *Phys. Rev. B* **2009**, *79*, 2354361–23543610.
- (22) Jing, C.; Fang, Y. Experimental (SERS) and theoretical (DFT) studies on the adsorption behaviors of L-cysteine on gold/silver nanoparticles. *Chem. Phys.* **2007**, *332*, 27–32.
- (23) Diaz Fleming, G.; Finnerty, J. J.; Campos-Vallette, M.; Célis, F.; Aliaga, A. E.; Fredes, C.; Koch, R. Experimental and theoretical Raman and surface-enhanced Raman scattering study of cysteine. *J. Raman Spectrosc.* **2009**, *40*, 632–638.
- (24) Santos, E.; Avalle, L. B.; Scurtu, R.; Jones, H. L-Cysteine films on Ag(111) investigated by electrochemical and nonlinear optical methods. *Chem. Phys.* **2007**, *342*, 236–244.
- (25) Santos, E.; Avalle, L.; Pötting, K.; Vélez, P.; Jones, H. Experimental and theoretical studies of L-cysteine adsorbed at Ag(111) electrodes. *Electrochim. Acta* **2008**, *53*, 6807–6817.
- (26) Perdew, J. P.; Chevary, J. A.; Vosko, S. H.; Jackson, K. A.; Pederson, M. R.; Singh, D. J.; Fiolhais, C. Atoms, molecules, solids, and surfaces: Applications of the generalized gradient approximation for exchange and correlation. *Phys. Rev. B* **1992**, *46*, 6671–6687.
- (27) Soler, J. M.; Artacho, E.; Gale, J. D.; García, A.; Junquera, J.; Ordejon, P.; Sánchez-Portal, D. The SIESTA method for ab initio order-N materials simulation. *J. Phys.: Condens. Matter* **2002**, *14*, 2745–2781.
- (28) Soler, J. M.; Artacho, E.; Gale, J. D.; García, A.; Junquera, J.; Ordejon, P.; Sánchez-Portal, D. <http://uam.es/departamentos/fismateria/c/siesta/>.
- (29) Troullier, N.; Martins, J. L. Efficient pseudopotentials for plane-wave calculations. *Phys. Rev. B* **1991**, *43*, 1993–2006.
- (30) Kokalj, A.; Dal Corso, A.; de Gironcoli, S.; Baroni, S. The Interaction of Ethylene with Perfect and Defective Ag(001) Surfaces. *J. Phys. Chem. B* **2002**, *106*, 9839–9846.
- (31) Kokalj, A. Computer graphics and graphical user interfaces as tools in simulations of matter at the atomic scale. *Comput. Mater. Sci.* **2003**, *28*, 155–168; XCrySDen—a new program for displaying crystalline structures and electron densities. *J. Mol. Graphics Modell.* **1999**, *17*, 176–179. Code available from <http://www.xcrysden.org/>.
- (32) Heimel, G.; Romaner, L.; Zojer, E.; Brédas, J. L. Toward Control of the Metal-Organic Interfacial Electronic Structure in Molecular Electronics: A First-Principles Study on Self Assembled Monolayers of π -Conjugated Molecules on Noble Metals. *Nano Lett.* **2007**, *7*, 932–940.
- (33) Rangger, G. M.; Romaner, L.; Heimel, G.; Zojer, E. Understanding the properties of interfaces between organic self-assembled monolayers and noble metals – a theoretical perspective. *Surf. Interface Anal.* **2008**, *40*, 371–378.
- (34) Arce, M. D.; Quaino, P.; Santos, E. Electronic changes at the Pt(111) interface induced by the adsorption of OH species. *Catal. Today*. In press.
- (35) Groß, A. *Theoretical Surface Science—A Microscopic Perspective*; Springer: Berlin, 2002.
- (36) Görbitz, C. H.; Dalhus, B. L-Cysteine, Monoclinic Form, Redetermination at 120 K. *Acta Crystallogr., Sect. C: Cryst. Struct. Commun.* **1996**, *52*, 1756–1659.
- (37) Heinz, H.; Farmer, B. L.; Pandey, R. B.; Slocik, J. M.; Patnalk, S. S.; Pachter, R.; Naik, R. R. Nature of Molecular Interactions of Peptides with Gold, Palladium, and Pd-Au Bimetal Surfaces in Aqueous Solution. *J. Am. Chem. Soc.* **2009**, *131*, 9704–9714.